Stress enhanced gold dispersion by solvent induced crystallization in BPA-PC membranes

Jacek K. Stolarczyk[a,*], Zbigniew J. Grzywna[a], Krzysztof K.K. Koziol[a,b,1]

[a]*Department of Physical Chemistry and Technology of Polymers, Silesian University of Technology, Strzody 9, 44-100 Gliwice, Poland*
[b]*Faculty of Engineering, Chair for Multicomponent Materials, Christian-Albrechts University, Kaiserstrasse 2, 24143 Kiel, Germany*

Abstract

In this paper the embedding of gold clusters in crystallizing bisphenol-A polycarbonate is treated as diffusion with drift in inhomogeneous and changing in time medium. Initially the gold is deposited on the polymer surface, which is subsequently exposed to acetone vapour. The polymer undergoes significant crystallization, induced by diffusing agent, while gold clusters become embedded in its bulk. The paper presents a model of gold dispersion based on Smoluchowski equation. It identifies the driving force of dispersion with the gradient of stress field generated during crystallization. Numerical results of the model are found to be in good agreement with available experimental data obtained by XPS depth profiling technique.
© 2004 Published by Elsevier Ltd.

Keywords: Vapour induced crystallization; Gold dispersion; Diffusion

1. Introduction

The class of materials known as metal–polymer composites, where the metal constituent is interspersed in polymer matrix, hold promise for next generation materials [1]. They offer interesting optical, electrical, catalytic and other properties being in fact downsizing materials to a nanometre length scale.

Gold–polymer composites are of particular importance in catalysis because of gold low resistivity and inertness to chemical corrosion. As a result of its inherent chemical stability, gold may be used for applications, where reliability must be rigorously maintained. Commonly encountered applications of gold range from electrical contacts to integrated circuits and wiring in multi-chip packaging modules.

Wide interest in this field has lead to a number of experimental observations. Akamatsu and Deki [2] have shown that gold deposited on polymer surface becomes embedded in the bulk upon heating the polymer above its glass transition temperature. They have demonstrated that a (thermally induced) bulk crystallization is a prerequisite for the process. In a further development, acetone vapour has been used [3] to induce crystallization in bisphenol-A polycarbonate (BPA-PC), following earlier work on vapour/solvent induced crystallization (known as VINC/SINC) by Makarewicz and Wilkes [4], Kambour [5]. Penetrant sorption plastifies the polymer and lowers its glass transition temperature T_g, allowing for crystallization to commence at ambient temperature. In effect VINC was found to be an alternative to the heat treatment method of embedding. However, that still left open the question of the 'driving force' for the embedding of gold clusters into the bulk.

The paper attempts to provide a theoretical explanation of the observed phenomena. It builds upon previous works on solvent induced crystallization [6,7], spherulite growth theory [8] and diffusion in glassy polymers [9–13] to offer a possible mechanism of gold dispersion in BPA-PC.

The paper is organized as follows. The second chapter very briefly describes experimental results for acetone sorption and X-ray photoelectron spectroscopy (XPS) gold depth profile analysis. The experimental details for XPS and other techniques are given elsewhere [3]. Two alternative models for stress build-up and its influence on gold embedding are shown in Section 3 and their predicted

* Corresponding author. Tel.: +48-32-237-1427; fax: +48-32-237-1722.
  E-mail address: jacek@mer.chemia.polsl.gliwice.pl (J.K. Stolarczyk).
1 Present address: Department of Materials Science, Cambridge University, Pembroke Street, Cambridge, CB2 3QZ, UK.

results are given and discussed in Section 4. Section 5 concludes and summarizes the main results of the paper.

2. Experimental

A thorough description of the experimental setup and the results obtained is given elsewhere [3]. The 2 μm thick BPA-PC membrane was created by fast evaporation from solution in dichloromethane (DCM) and put on aluminum support. In the next step gold particles were deposited on the surface, the resulting systems composed of very small metal particles were found to be thermodynamically unstable, though. Gold does not wet the polymer surface hence the metal particles tend to grow spherical clusters (Volmer–Weber type of growth). Microscopic observations by AFM and transmission electron microscopy (TEM) allowed for estimating the sizes of the clusters as 10–13 nm (AFM) and 6–10 nm (TEM).

Later the membrane was exposed to acetone vapour. Acetone sorption is known to swell polycarbonate and the penetrant diffusion exhibits Case II behaviour [7,11]. The sorption experiments were performed separately on 1.65 ± 0.05 mm thick film (to properly record kinetics). Fig. 1 shows the plot of mass uptake vs. time (unsymmetrical sorption [14]). The acetone mass increases linearly with time (for early times) confirming the Case II mechanism of diffusion. Sorption into thin membranes (2 μm) followed a similar pattern (but results were less accurate), in agreement with literature reports [7,15,16]. Therefore taking sorption measurements on thicker membranes seems to be possible in this case.

The induction time identified as a characteristic feature of Case II behaviour by Thomas and Windle [12] is also visible in Fig. 1 and is equal to about 300 s. An inward moving penetrant front separating glassy core from the outer, swollen layers has been reported in literature [5,7,12]. Hence we assumed that at early times linear acetone uptake corresponds to a front moving with constant velocity v and a
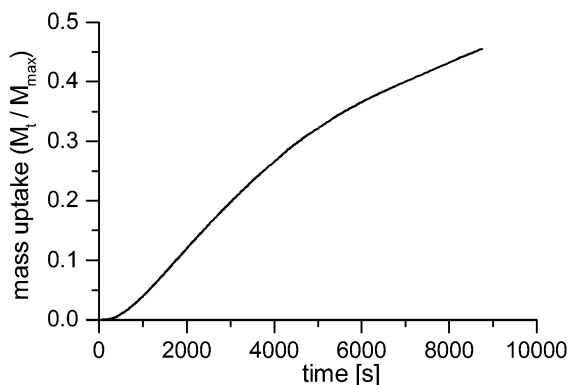
fully saturated polymer (no concentration gradient) behind the front. Taking such an assumption the front velocity equals 0.103 [μm/s].). Additionally, the volume fraction of acetone, which is equal 0.194, has been calculated from absolute values of the final mass uptake (59.682 mg).

A surface gold signal (line 4f) from XPS technique decreased with time suggesting that the gold clusters were gradually becoming embedded into the polymer bulk (see Fig. 2). Therefore XPS, combined with 'ion beam sputtering', was used to obtain gold depth profiles. A profile obtained after 35 h (see Fig. 3) shows a distinctive peak in the gold concentration about 100 nm below the surface.

The sputtering is destructive to the sample thus the experimental results need to be obtained from a series of samples, additionally spoiling the reliability of kinetic data. However, it is clear that the peak in gold concentration moves into the bulk, reaching as far as 200 nm in available data, about one tenth of the membrane thickness.

3. Model of gold embedding

3.1. Model development

As already mentioned, Akamatsu and Deki [2] associated the embedding of gold clusters with crystallization of the polymer, but no 'driving force' has been identified. In a way of filling this gap we can observe there are two stages of embedding which need distinguishing. In the initial stage (see Fig. 2) a small fraction of gold clusters is found several nanometres inside the bulk but the rest remains on or just below the surface. Three effects may explain this phenomenon:

- High density gold clusters gravitationally dip into the plasticized polymer. The heavier/larger the clusters the deeper they become embedded.
- Gibbs free energy of a metal particle inside a polymer is lower than that of a particle on the surface. It is related to the high cohesive energy of metals which gives rise to a

Fig. 1. Early times of acetone vapour sorption into BPA-PC film as a function of time. The total mass uptake M_{max} was 59.682 mg [3].
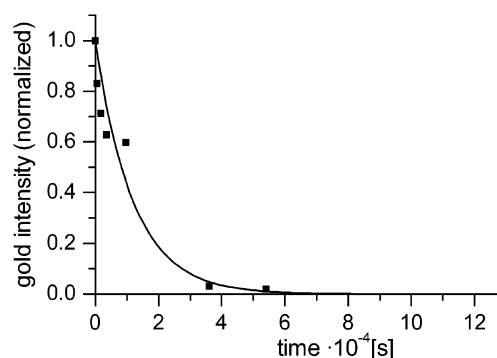

Fig. 2. A decrease of 4f gold line signal in time upon the exposure of BPA-PC films to the vapour of acetone [3] (squares) and numerically fitted exponential decay (solid line).
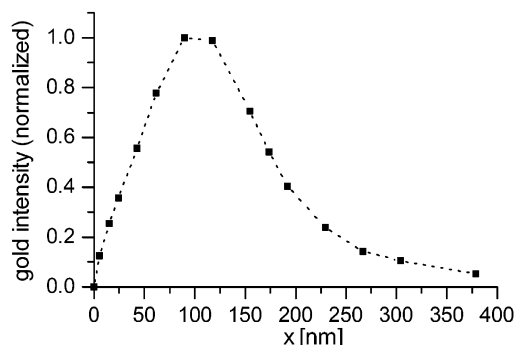
Fig. 3. XPS gold depth profile in BPA-PC film covered with 1.5 nm (nominal thickness) of gold, exposed for 35 h 30 min. to the vapour of acetone [3].

correspondingly high surface Gibbs free energy of gold. The surface free energy may be reduced by embedding if the surface tension γ_M of the metal particles exceeds the sum of the interfacial tension γ_{MP} and the polymer surface tension γ_P :

$$\gamma_M > \gamma_{MP} + \gamma_P \tag{1}$$

- The observed initial gold distribution may be a result of the inaccuracy of the method (due to presence of Au clusters on the surface).

At long times gold depth profiles exhibit apparent single peaks in the distribution moving into the bulk (Fig. 3) which cannot be explained in terms of the above mentioned effects. Two other explanations, quite natural in this situation, do not seem feasible either:

- A classical diffusion-like process does not seem possible due to the large size of the gold clusters. It is evident from TEM measurements that the gold appears in the membrane in the forms of clusters, not atoms [3]. Furthermore, a positive gradient of gold for $x < x_{peak}$ (where x is a coordinate perpendicular to the surface) would attenuate the peak rather than preserve it.
- Crystallization front (visible as a polymer loses its transparency and becomes translucent or opaque) which moves into the bulk and pushes gold clusters ahead of itself. The movement of such a front does not involve movement of the matter though (only changing its state), hence no such 'pushing' is possible. Crystallization and dispersion occur on different time scales (15–30 min for crystallization and 15–40 h for dispersion [3,11]) so they must follow different kinetics. With the crystallization front approach, one would also expect gold clusters to reach the other side of the film, as the whole membrane crystallizes. That appears not to be the case here, gold reaches only a small fraction of its thickness.

The model, which could be successfully applied to the observed phenomena, needs to predict their two main features: net movement of gold into the bulk and gradual broadening of the initially delta-like profile.

3.2. Model A: diffusive front arrival time

It is known that diffusion of small particles into glassy polymers can induce significant internal stresses [9,12,17]. It is generally understood, however, that they relax when the polymer swells and goes through a glass transition into a rubbery state (gel). We believe that crystallization can again induce stresses in the otherwise plasticized polymer (especially on the tie molecules). Growing spherulites would exert that stress on the penetrant and gold particles, however, only the effect on the latter would be of interest to us (Fig. 4). It may be assumed, that the spherulites grow isotropically, enabling us to treat that induced stress as pressure, similarly to the approach presented by Argon et al. [17]. Hence, even though the symbol σ is called 'the stress' throughout the paper, it actually refers to the pressure component of the local stress tensor, which by definition, is a negative mean normal stress $\sigma_m = (\sigma_{11} + \sigma_{22} + \sigma_{33})/3$. We also use an analogy to Cohen et al. [18] approach for diffusion induced stresses to derive the equation for its development. Cohen used a combination of Maxwell and Voigt models of viscoelastic responses and assumed the dependence on strain and strain rate might be replaced by a dependence solely on the penetrant concentration and its rate of change.

$$\frac{\partial \sigma}{\partial t} + \beta\sigma = g\left(c, \frac{\partial c}{\partial t}\right) \tag{2}$$

In most cases they used an even simpler approach leaving out the rate term and taking a linear dependence on c. Accordingly we assume that the rate of change of stress may be related to the volume fraction crystallized f in a similar fashion.

$$\frac{\partial \sigma}{\partial t} + \beta\sigma = g(f) = af \tag{3}$$

The model of kinetics of solvent induced crystallization was developed by Durning [7] with two coupled equations for penetrant diffusion and crystallization. However, in the case
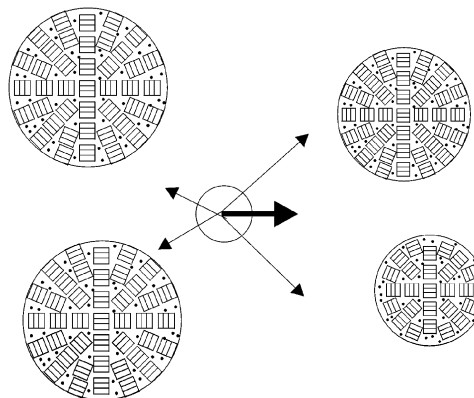

Fig. 4. Schematic drawing of stress exerted on gold cluster by growing spherulites.

of acetone–BPA-PC system the diffusion is much faster than crystallization [11]. Two equations decouple and the diffusion process may be represented (early times) by a 'travelling wave' form of solution, following the observed Case II sorption kinetics:

$$\begin{cases} c_{Ac}(x,t) = 0 & \text{for } t < x/v \\ c_{Ac}(x,t) = c_{Ac}^{e} & \text{for } t > x/v \end{cases} \tag{4}$$

where c_{Ac} is a volume fraction of acetone and c_{Ac}^{e} is a equilibrium volume fraction of acetone in PC, obtained from mass uptake measurements. The gold dispersion is much slower than crystallization, hence we believe that the effect of Au clusters on crystallization kinetics is negligible. The crystallization kinetics equation is taken from Durning's model [7]:

$$\begin{cases} \dfrac{\partial f}{\partial t} = \Omega h_1(c_{Ac}) f^{2/3}(f_0 - f) \\ f(x,t) = f^0 & \text{for } t < x/v \end{cases} \tag{5}$$

Ω is a nondimensional rate of crystallization, $h_1(c_{Ac})$ rate of spherulite growth [10], f_0 is a final volume fraction of crystallized phase and f^0 is the initial crystallization fraction. We assume there is no gradient behind the diffusion front (see Eq. (4)) so the $h_1(c_{Ac})$ function is basically a constant (corresponding to $h(\gamma = 1)$ in Durning's general approach). Eq. (5) is integrated starting from the time when the diffusion front arrives. The front advances with constant velocity v (and obviously the deeper into the bulk the later it arrives), thus a gradient in f is created (see Fig. 5).

The sample stress gradient calculated from Eq. (2) is shown in Fig. 6.

3.3. Model B: desorption of acetone

While the model presented above (A) provides an acceptable mechanism for stress gradient occurrence in the membrane, its drawbacks have to be seriously analyzed. Firstly it takes about 20 s for the diffusive front to advance through the membrane, yet the model assumes that the
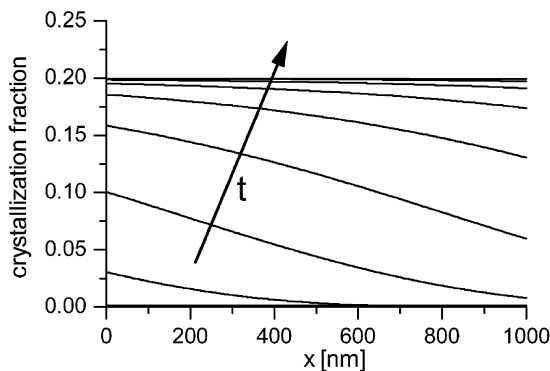
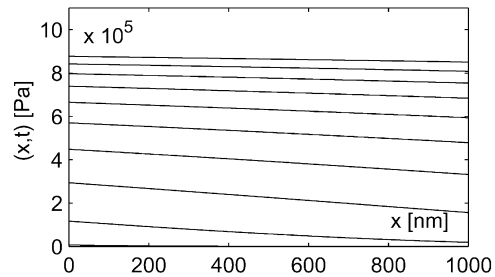Fig. 5. Evolution of fraction of crystallized phase profiles (parameter values given in text).

Fig. 6. Evolution of stress field profiles (parameter values given in text).

differences in stress throughout the membrane last for hours. Given also the induction time of crystallization (about 1 min [11]), that assumption appears unlikely. Anyway, such a model may be probably successfully applied to systems with significantly slower diffusion compared to crystallization (acetone + poly(ethylene terephtalate) [7]). Secondly, the crystallizing polymer is still strongly plasticized by the penetrant, so the rate of stress relaxation should still be high.

It is generally agreed, however, that the relaxation time grows during the desorption of the penetrant from the membrane. The penetrant is initially desorbed only from the exposed surface layers, followed by the deeper layers. Hence the possible source of stress gradient appears. The obvious question that should be answered, is why the desorption would commence in the first place, since the membrane is kept under the constant temperature and penetrant vapour pressure.

When the membrane is exposed to acetone vapour, the sorption relatively quickly (in minutes) leads to an equilibrium concentration of the acetone c_{Ac}^{e} inside the membrane. However, the crystallization leads to extrusion of the acetone molecules from the growing crystallites, and this creates its nonequilibrium excess concentration c_{Ac}^{0} in the amorphous phase. The acetone has to partially desorb to equilibrate the system once again. The desorption from the crystallizing polymer should be slower than from the amorphous one, and strongly hampered by the Au clusters in the vicinity of the surface. Therefore the desorption and gold dispersion may occur at similar time scales, a phenomenon the earlier model could not predict.

Acetone desorption is modelled by a simple diffusion equation:

$$\begin{cases} \dfrac{\partial c_{Ac}}{\partial t} = D_{Ac} \dfrac{\partial^2 c_{Ac}}{\partial x^2} & \text{for } x > 0 \\ c_{Ac}(x,0) = c_{Ac}^{0} \\ c_{Ac}(0,t) = c_{Ac}^{e} + (c_{Ac}^{0} - c_{Ac}^{e})\exp(-t/\beta) \end{cases} \tag{6}$$

where $c_{Ac}^{0} > c_{Ac}^{e}$. Following Argon et al. [17] we used the modified Maxwell model of viscoelasticity with strain rate proportional to the rate of change of acetone concentration c_{Ac}:

$$\frac{\partial \sigma}{\partial t} + \beta\sigma = a\frac{\partial c_{Ac}}{\partial t} \tag{7}$$

3.4. Smoluchowski equation

The stress field (Fig. 6) may be treated in Hooke's law regime as a potential field. The force acting on a body in that field is proportional to its gradient:

$$F = -\alpha \cdot \nabla \sigma \tag{8}$$

In our case it reduces to a one-dimensional equation:

$$F = -\alpha \frac{\partial \sigma}{\partial x} \tag{9}$$

We treat the plasticized polymer as a viscous medium, which reacts to the motion of a sufficiently large object (like a gold cluster) according to Stokes law:

$$F = 6\pi \eta \upsilon r \tag{10}$$

where η is a viscosity of a polymer 'solution', υ is a velocity of a spherical object of radius r. From Eqs. (9) and (10) we derive a formula for the average velocity of a gold cluster:

$$\upsilon = -\frac{\alpha}{6\pi \eta r} \frac{\partial \sigma}{\partial x} \tag{11}$$

Spherulites do not grow uniformly in the polymer bulk, thereby creating an inhomogeneous environment on the local scale. Therefore on such a scale local stress gradients significantly affect the motion of gold clusters. They move in all directions (or back and forth in one dimension), even though the net result is a slow inward movement due to the global stress gradient. The apparent randomness of this motion, which may be attributed to the random nucleation of crystallites in a polymer, resembles the characteristic behaviour of a Brownian random walk. Thus a diffusion coefficient D may be associated with this motion.

The dispersion of gold clusters may be now explained in terms of diffusion in a potential stress field. Dispersive transport in an external force field has been studied earlier by Metzler and Klafter [19]. The theoretical background with the derivation form the random walk approach has been provided by the authors of the paper elsewhere [20]. In the present case the process of diffusion does not come as a result of fluctuations of polymer chains (which are becoming stalled during crystallization)—we claim the gold clusters are too large for them to have a measurable effect. Rather we think it is induced by a local variance of stress gradient developed by an inhomogeneous growth of spherulites, as described above. It is worthy to notice that diffusion of gold atoms (not clusters) has been analyzed previously, but in a different environment (BPA-PC close to and above T_g) [21]. Diffusion in a potential field is effectively modelled (was modeled) by Smoluchowski equation, with time dependent parameters:

$$\frac{\partial c}{\partial t} = D(t) \frac{\partial^2 c}{\partial x^2} - \upsilon(t) \frac{\partial c}{\partial x} \tag{12}$$

Crystallization significantly changes the environment, thus in general the diffusion coefficient should be a function of time (it decreases in crystallizing polymer).

Similarly velocity υ, which is a function of viscosity Eq. (11) also decreases during crystallization, because the viscosity increases (was: which increases during crystallization). The simplified problem with a constant diffusion and viscosity coefficient is solved elsewhere [20]. Hence we pose the problem as follows:

$$\begin{cases} \dfrac{\partial c}{\partial t} = D(t) \dfrac{\partial^2 c}{\partial x^2} - \upsilon(t) \dfrac{\partial c}{\partial x} & \text{for } x \in (0, L) \\ c(x, 0) = c^0(x) \\ c(0, t) = c_0(t) \\ c(L, t) = 0 \end{cases} \tag{13}$$

where $c^0(x) < c_0(t)$. In fact we could have also used a semi-infinite domain for the problem, mostly because of the time scale considered, as well as the stress relaxation.

There could possibly be one more viable source of the observed broadening (other than diffusion) of the gold depth profile–size segregation. Stress would act differently on clusters depending on their size, some of them reaching further than others do. However, imaging of clusters inside the polymer by TEM [3] does not show any size segregation. Moreover when a Monte Carlo simulation was run for Gauss distribution of clusters' sizes the resulting gold profiles significantly differed from experimental ones. We therefore treated the clusters as uniformly sized, still we acknowledge that the effect of size definitely could contribute to gold dispersion to some minor degree.

3.5. Model parameters

The left boundary condition $c_0(t)$ was calculated from the XPS surface gold intensity experiments. Experimental data were modelled by a single exponential decay function $\exp(-t/\lambda)$. Nonlinear regression yielded $\lambda = 1.19 \times 10^4$ [s] (solid line in Fig. 2). The initial condition was also approximated in similar fashion by a single exponential $c^0(x) = \exp(-x/7.4769 \times 10^{-9})$ from the initial experimental gold profile (see Fig. 7).

The average sizes of gold clusters have been estimated from AFM and TEM images as 10–13 nm (AFM) and 6–10 nm (TEM) in diameter. We used 9.8 nm in further calculations. Membrane's thickness was 2 μm, diffusion front velocity was calculated in chapter 2 as 0.103 [μm/s], equilibrium volume fraction of acetone $c_{Ac}^e = 0.194$. Two values were taken from the derivation of the Durning model [7] for BPA-PC–acetone system: $\Omega = 3$ and $f_0 = 0.2$ (given also in Ref. [11]).

Data for estimating viscosity of BPA-PC plasticized by acetone were not readily available. Thus we followed the exponential dependence on concentration suggested by Thomas and Windle [12] ($\eta = \eta_0 \exp(-Mc_{Ac})$). Using the values of $\eta_0 = 1.5 \times 10^{14}$ [Pa s] and $M = 13$ we arrived at
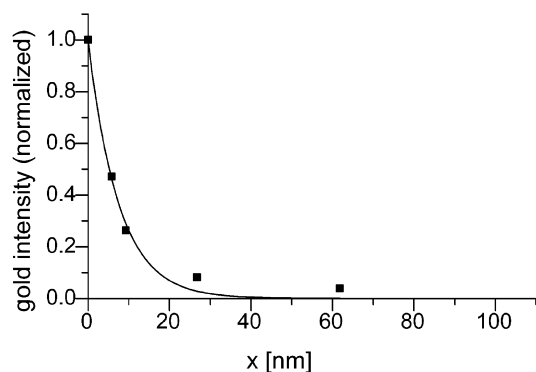
Fig. 7. XPS gold depth profile in BPA-PC film covered with 1.5 nm (nominal thickness) of gold, no exposure to the vapour of acetone (squares) [3], and numerically fitted exponential decay (solid line).
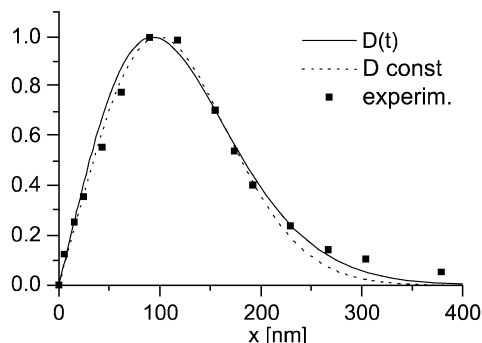

Fig. 8. Comparison of simulation results for exponentially decaying D and exponentially growing η (solid line, time, 34.75 h), simulation results for constant $D = 4.8 \times 10^{-18}$ [m^2/s] (dotted line, time, 34.75 h) and XPS experimental depth profile (squares, time, 35 h). Parameter values are given in text.

the value $\eta = 1.2 \times 10^{13}$[Pa s]. Growth of the spherulites parameter $h_1(c)$ was estimated as 1.8×10^{-4}, a value that matched the crystallization kinetics observed experimentally. Two parameters were adjustable: a—coefficient for stress development and α—proportionality coefficient between the stress gradient and the force acting on a cluster. Actually they may be reduced to one parameter (as they are in fact multiplied by themselves), but were left separate because it should be possible to estimate a from relaxation experiments and absolute values of stresses. Inverse relaxation time of crystallizing polymer (β) was taken the value 2.0×10^{-5} [1/s] ($\tau_r \cong 14$ h). The remaining parameters are given in the next chapter.

4. Results and discussion

4.1. Front arrival time

The model A has been already shown to produce good fit to the experimental data [20], even for constant diffusion and viscosity coefficient. Still taking more physically acceptable decreasing D and increasing the viscosity coefficient allowed us to achieve an even better fit. The model (13) was solved numerically using fully implicit formula. Fig. 8 presents the development of gold depth profiles for 35 h—same duration as with experimental data (Fig. 3), for $a = 100$, $\alpha = 2.1 \times 10^{-15}$. Exponential relations have been assumed for D and η: $D(t) = 3.55 \times 10^{-17} \exp(-t/2.5 \times 10^4)$[m^2/s] and $\eta(t) = 1.2 \times 10^{13} \exp(t/2.5 \times 10^4)$[Pa s].

An almost perfect agreement is seen between both results. Only the tails (for deeper layers of the membrane) differ slightly. While this may well be attributed to experimental accuracy (sputter background [21]), there seem to be a few other explanations:

- the dependence on the distribution of sizes, discussed above, (Levy distribution), which was neglected
- void formation—it is well known that voids form during

crystallization [7]. When a cluster moves into the void its velocity v increases (due to smaller viscosity). This way some gold clusters may effectively go further into the bulk.

4.2. Desorption of acetone

The equilibrium concentration of acetone (volume fraction) was estimated on sorption data to equal about 0.2. Given that also about 0.20 of the volume is subsequently taken by the crystallites, the excess concentration is estimated to be 0.25. That allowed to solve the model of desorption of acetone (6), the results of which are presented in Fig. 9:

Coefficient of diffusion in this model was taken as $D_{Ac} = 1.0 \times 10^{-17}$[m^2/s], with $\beta = 5.0 \times 10^4$[1/s]. It is clearly visible that the concentration of acetone gradually decreases to the equilibrium value, creating a penetrant concentration gradient inside the membrane. Hence the stress field was calculated from Eq. (7) (see Fig. 10).

There exists initially a gradient of stress, which may cause the inward motion of gold clusters. The gradient later reverses, due to the stress relaxation, but by that time the environment is effectively 'frozen' because of crystallization and growth of viscosity. Therefore no outward motion is observed.

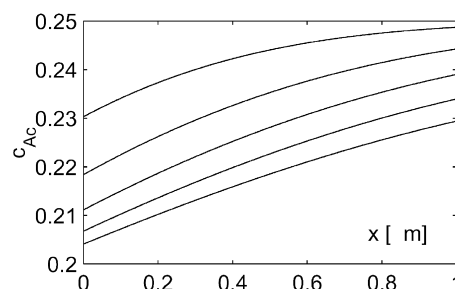The model of gold dispersion has been solved in similar

Fig. 9. Simulation of concentration of acetone inside the membrane. Lines for $t = 0$ s, $t = 2.5 \times 10^4$ s, $t = 5.0 \times 10^4$ s, $t = 7.5 \times 10^4$ s, $t = 10.0 \times 10^4$ s, $t = 12.5 \times 10^4$ s, (34.75 h).
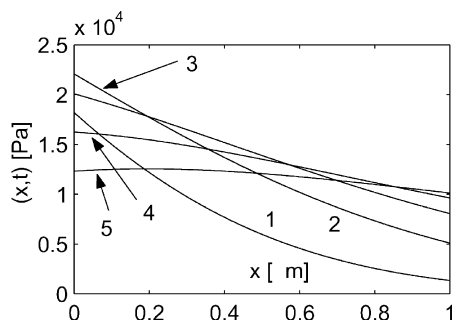
Fig. 10. Evolution of stress profiles. Lines for $t = 0$ s, $t = 2.5 \times 10^4$ s, $t = 5.0 \times 10^4$ s, $t = 7.5 \times 10^4$ s, $t = 10.0 \times 10^4$ s, $t = 12.5 \times 10^4$ s (34.75 h).

manner as previously, for $D(t) = 8.00 \times 10^{-20} \exp(-t/2.5 \times 10^4)[\text{m}^2/\text{s}]$ and $a = -1.2 \times 10^6$. Other parameters have been assigned the same values as previously.

Fig. 11 shows a very good agreement between experimental data (after 35 h) and the solution of the model. The integral of that curve (mass of Au inside the membrane) is presented in Fig. 12. Initially the mass of gold increases due to the clusters on the surface or its vicinity being forced into the polymer bulk. At later times some of these clusters again diffuse out of the membrane. That observation has not yet been confirmed (nor dismissed) experimentally and awaits further checking. They seem to further slow down desorption of acetone—another reason why acetone desorption and gold dispersion can occur on the same time scales.

5. Concluding remarks

Gold deposition and subsequent embedding in polymer matrices is an important step in the production of novel materials ranging from nanocomposites through microelectronic devices to endurable compact disks. Gold profiles showing maxima at specific depths promise new applications, e.g. in electronic circuits. Experimental results suggest that both thermally and vapour induced crystallization could cause embedding.

The overall experiment involves three processes occurring at different time scales: diffusion of penetrant (fastest),
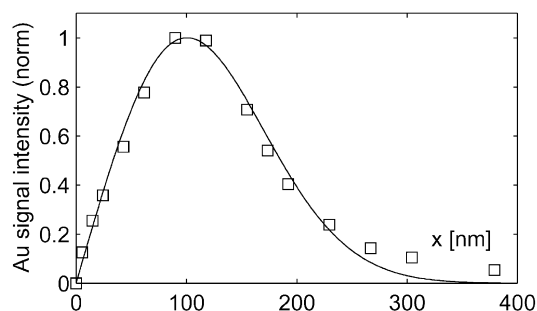

Fig. 11. Comparison of simulation results (solid line, time, 34.75 h) with XPS experimental depth profile (squares, time, 35 h). Parameter values are given in text.
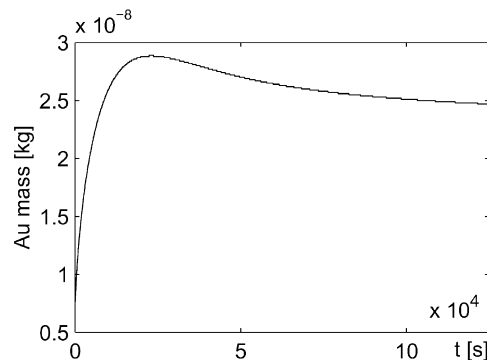

Fig. 12. Gold mass uptake during the dispersion.

induced crystallization and gold embedding (slowest). During an experiment the environment undergoes significant structural changes leading to the development of stresses. The global gradient of stresses seems to be responsible for the convective term in the Smoluchowski equation while local inhomogeneities induced by growing spherulites account for the diffusive term. Two models based on such assumptions successfully predict experimental XPS profiles. The models allow also prediction of the kinetics of dispersion—data difficult to validate as the experimental data is too scarce. Especially valuable would be checking whether the peak indeed slows its movement or proceeds further.

While both models result in a good fit to the experimental data, the second one seems to have a sounder theoretical background, and does not need rather unrealistic assumptions on the time scales of the processes. Because of the simple nature of the experimental curve we cannot accept a model only because of the fit. It is, however, an indication, that a more general model, merging features of both models presented in the paper, could also be used to model the dispersion of nanoclusters in a broader family of systems, including different polymers like poly(ethylene terephtalate).

Acknowledgements

References

[1] Nalwa HS. Nanostructured materials ans nanotechnology, 1st ed. New York: Academic Press; 2001.
[2] Akamatsu K, Deki S. Nanostruct Mater 1997;8:1121–9.
[3] Stolarczyk J. Diffusion in polymers in diffusion-induced stress field. PhD Thesis. Silesian University of Technology, Gliwice; 2002. Experimental part (done at Kiel University) covered in detail by

Koziol K. Dispersion of noble metal nanoclusters in bisphenol-(A)-polycarbonate by acetone vapour diffusion and polymer crystallization. MSc Thesis. Silesian University of Technology, Gliwice; 2001.

[4] Makarewicz PJ, Wilkes GL. J Polym Sci Polym Phys Ed 1978;16: 1529–42.

[5] Kambour RP, Gruner CL, Romagosa EE. Macromolecules 1974;7: 248–53.

[6] Zachmann HG, Konrad G. Makromol Chem 1968;118:189.

[7] Durning CJ, Russel WB. Polymer 1985;26:119–30.

[8] Makarewicz PJ, Wilkes GL. J Polym Sci Polym Phys Ed 1978;16: 1559–82.

[9] Alfrey T, Gurney EF, Lloyd WG. J Polym Sci Part C 1966;12: 249–61.

[10] Friedman A, Rossi G. Macromolecules 1997;30:153–4.

[11] Turska E, Janeczek J. Polymer 1979;20:355.

[12] Thomas NL, Windle AH. Polymer 1982;23:529–42.

[13] Frisch HL. Polym Engng Sci 1980;20:2–13.

[14] Crank J. Mathematics of diffusion, 2nd ed. Oxford: Clarendon Press; 1975.

[15] Jones RAL. Curr Opin Colloid Interf Sci 1999;4:153–8.

[16] DeMaggio GB, Frieze WE, Gidley DW, Ming Z, Hristov AF, Yee AF. Phys Rev Lett 1997;78:1524–7.

[17] Argon AS, Cohen RE, Patel AC. Polymer 1999;40:6991–7012.

[18] Cohen DS, White AB. SIAM J Appl Math 1991;51:472–83.

[19] Metzler R, Klafter J. J Mol Liquids 2000;86:219–28.

[20] Grzywna ZJ, Stolarczyk J. Int J Mod Phys Part C 2002;13:1301–12.

[21] Willecke R, Faupel F. Macromolecules 1997;30:567–73.